Anisotropy of the temperature dependence of electrical resistivity in aluminium single crystals

1994 J. Phys.: Condens. Matter 6 L637

(http://iopscience.iop.org/0953-8984/6/43/001)

J. Phys.: Condens. Matter 6 (1994) L637–L642. Printed in the UK

LETTER TO THE EDITOR

Anisotropy of the temperature dependence of electrical resistivity in aluminium single crystals

Y Ueda, H Tamura and E Hashimoto

Laboratory of Crystal Physics, Faculty of Science, Hiroshima University, Higashi-Hiroshima 724, Japan

Received 30 August 1994

Abstract. The anisotropy of the temperature-dependent part of the electrical resistivity has been measured in the range 4.2–80 K on aluminium single crystals with a common surface orientation {110} and specimen axes ⟨100⟩, ⟨111⟩ and ⟨110⟩. The specimens were cut from one single-crystal rod with a residual resistance ratio of about 50 000. The temperature-dependent part of the ⟨100⟩ specimen, $\rho_{100}^{ph}(T)$, is larger than that of the ⟨111⟩ specimen, $\rho_{111}^{ph}(T)$, below about 25 K. Then, $\rho_{100}^{ph}(T)$ becomes smaller than $\rho_{111}^{ph}(T)$ above that temperature. At higher temperatures, the anisotropy gradually disappears. On the other hand, the temperature-dependent part of the ⟨110⟩ specimen, $\rho_{110}^{ph}(T)$, is smaller than $\rho_{111}^{ph}(T)$ at low temperatures and this anisotropy vanishes rapidly at higher temperatures. A mechanism for the anisotropy that arises from the anisotropic distribution of conduction electrons in an electric field applied along ⟨100⟩ is suggested.

Recently, we have reported experimental results that manifest the anisotropy of residual electrical resistivity in high-purity aluminium single crystals at 4.2 K [1]. Prior to studying the present subject of the temperature dependence, we briefly describe the results of this anisotropy of residual resistivity.

Figure 1 shows the experimental values of the resistivity $\rho(4.2\ \mathrm{K})$, obtained so far, as a function of $P/2A$, where P is the perimeter of a cross section and A the sectional area of a specimen. The main surface, about 3 mm in width, is cut parallel with {100} for all the specimens, prepared from one single-crystal rod with the residual resistance ratio RRR $\equiv R(300\ \mathrm{K})/R(4.2\ \mathrm{K})$ of about 50 000. The specimen axis along which a current flows is directed in one of three principal orientations ⟨100⟩, ⟨111⟩ and ⟨110⟩. The dependence of $\rho(4.2\ \mathrm{K})$ on the orientation of the specimen axis is distinct for $P/2A < 3 \times 10^3\ \mathrm{m}^{-1}$: the resistivity increases in the order of ⟨110⟩, ⟨111⟩ and ⟨100⟩ directions. The anisotropy of $\rho(4.2\ \mathrm{K})$ decreases in thin specimens in which the scattering rate of conduction electrons at the specimen surface is large. As the thickness of the specimens decreases, the $\rho(4.2\ \mathrm{K})$ values of the ⟨111⟩ and ⟨100⟩ specimens rapidly approach the $\rho(4.2\ \mathrm{K})$ value of the ⟨110⟩ specimens for $P/2A > 3 \times 10^3\ \mathrm{m}^{-1}$ and $> 4 \times 10^3\ \mathrm{m}^{-1}$, respectively, reducing their increment with $P/2A$. These results suggest that the anisotropic distribution of electrons in an applied electric field is homogenized by the increased surface scattering.

If the anisotropy of $\rho(4.2\ \mathrm{K})$ with the axis orientations arises from a break of the cubic symmetry due to impurities aligned in a certain direction or due to defects and microstructure produced in the surface layers during spark-cutting, the anisotropy will remain constant or increase in thin specimens. As the thickness of the specimens decreases, the volume fraction of the defects and microstructure becomes large, resulting in the increased resistivity.

0953-8984/94/430637+06$19.50

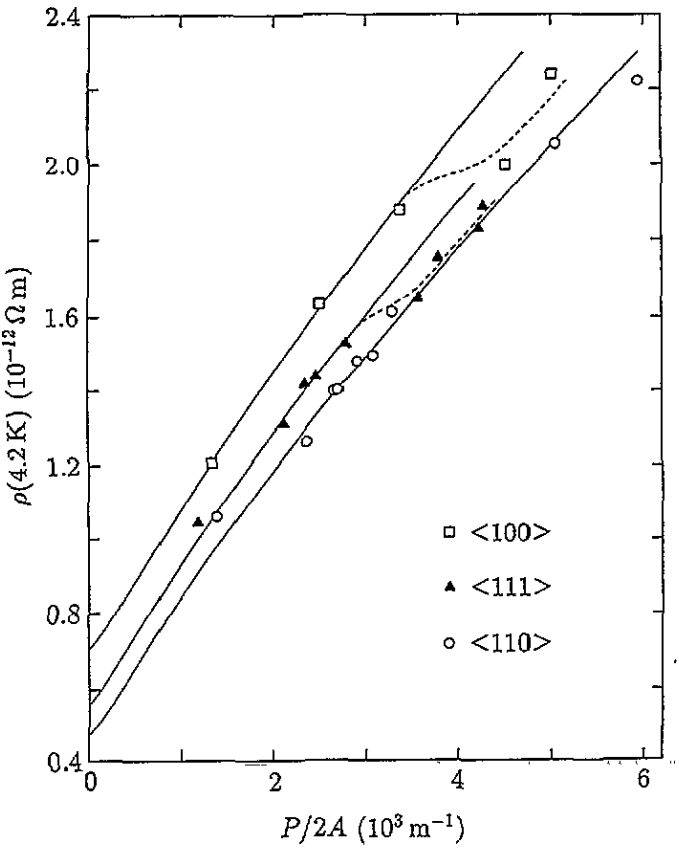

Figure 1. Experimental values of $\rho(4.2\ \mathrm{K})$ as a function of $P/2A$. Here, P is the perimeter of the cross section and A the sectional area of the specimen. The notation $\langle hkl \rangle$ represents the orientation of the specimen axis, and the orientation of the main surface is $\{110\}$ for all the specimens. Solid curves are obtained according to the Fuchs–Sondheimer theory assuming that $p = 0$ and $\rho_b l_b = 0.82\ \mathrm{f\Omega\ m^2}$. Dashed curves are drawn to guide the eyes.

Therefore, the result in figure 1 that the anisotropy decreases in thin specimens shows that the impurities, the defects and the microstructure are not the cause of this anisotropy.

Solid curves in figure 1 are drawn through the data points for each axis orientation according to the Fuchs–Sondheimer theory [2]. As the specimens have been etched with aqua regia and annealed in air at 300 °C, the surface of the specimens is rather rough. Therefore, the surface scattering of conduction electrons was assumed to be diffuse, i.e., the specularity parameter $p = 0$ [3]. A value of $0.82\ \mathrm{f\Omega\ m^2}$ was used for the product of bulk resistivity and bulk mean free path [3, 4]. Each of these curves gives a good fit to the data obtained, except those for the thin $\langle 100 \rangle$ and $\langle 111 \rangle$ specimens, and for the thickest $\langle 111 \rangle$ and $\langle 110 \rangle$ specimens.

In thick specimens, the surface scattering on the side surface becomes large. The side surface of the $\langle 100 \rangle$ specimen has the same $\{110\}$ orientation as the main surface. However, the $\langle 111 \rangle$ and $\langle 110 \rangle$ specimens have $\{112\}$ and $\{100\}$ side surfaces, respectively. These side surfaces may give a different size effect from that from the $\{110\}$ main surface. This effect must necessarily be pronounced in thick specimens. For example, the value

of $\rho(4.2\ \mathrm{K})$ for the thickest ⟨110⟩ specimen suggests that the size effect due to the {100} surface is significantly larger than that due to the {110} surface. This is consistent with previous experiments on the anisotropic size effect in thin aluminium films [5]. If such a contribution from the side surface is negligible to the total resistivity, the Fuchs–Sondheimer theory with a suitable value of $\rho_b l_b$ as described above will be plausible to estimate the bulk residual resistivity, $\rho_b(4.2\ \mathrm{K})$, for the specimen studied.

The salient feature of the results shown in figure 1 is the anisotropy of the bulk residual resistivity $\rho_b(4.2\ \mathrm{K})$. The resistivity increases in the order of the ⟨110⟩, ⟨111⟩ and ⟨100⟩ directions: the values along ⟨100⟩ and ⟨111⟩ are 50% and 20% larger than that along ⟨110⟩, respectively. This result is noteworthy for the transport phenomena of electrons because aluminium is a normal metal and has cubic symmetry. For this reason, it has been generally believed that the resistivity is isotropic [6].

As far as the system is cubic and Ohm's law $\boldsymbol{i} = \boldsymbol{\sigma} \cdot \boldsymbol{E}$ stands, the conductivity tensor $\boldsymbol{\sigma}$ becomes a scalar and the resistivity is isotropic. In order to examine the appearance of the anisotropic resistivity due to the deviation from Ohm's law, we further measured the current–voltage characteristics on specimens for three principal axes and for a current from 0.08 A up to 1.2 A at 4.2 K. The voltage was measured with a superconducting chopper amplifier [7] with the optimum resolution of 2 pV. The linearity of an electric field E against a current density i was confirmed within the experimental error for all the specimens. Thus the anisotropy of the resistivity is not the non-linear effect of the current–voltage characteristics. The above linear behaviour also means that the possibilities of the influence of Joule heat and magnetoresistance that increases as i^2 are discarded. Therefore, we conclude that the anisotropy of $\rho_b(4.2\ \mathrm{K})$ obtained in this work is the intrinsic bulk property under the influence of the electric field.

As described above, the anisotropy of $\rho(4.2\ \mathrm{K})$ decreases in this specimens in which the scattering rate of conduction electrons at the specimen surface is large. The scattering rate of conduction electrons also increases with increasing temperature. Therefore, it is expected that anisotropic behaviour, similar to that found for $\rho(4.2\ \mathrm{K})$ as a function of $P/2A$, exists for the temperature dependence of the resistivity. In this letter, we present measurements of the temperature dependence of the resistivity in high-purity aluminium single crystals in order to study the mechanism of the anisotropy of electrical resistivity. Extensive investigations of the electrical resistivity and its temperature dependence have been made on pure aluminium [3, 8]. However, the anisotropy of resistivity as a bulk property is not reported in these previous works.

The measurements of the temperature dependence were performed on two sets of single-crystal specimens with the $(1\bar{1}0)$ surface about 0.5 mm × 3 mm in cross section and 15–30 mm in length. Each set consists of three specimens with the principal axes [110], [111] and [001] parallel to a current direction, respectively. These specimens were cut with a spark erosion machine from the close part of one aluminium single-crystal rod produced by zone refining. The residual resistance ratio RRR of this rod was about 50 000 in the bulk value and its growth direction was nearly parallel with the orientation [112]. The surface normal and the axis of the specimens were accurate within ±1°. The specimens were chemically etched with aqua regia and rinsed with distilled water to remove contaminations and damaged layers on the surface. Four zone-refined aluminium wires 0.3 mm in diameter were spot-welded on the specimens as the electrodes for the standard DC four-probe measurement. The potential contacts were placed sufficiently far inside to avoid the end effect. All the specimens were annealed in air at 300 °C for 3 h, and furnace-cooled to room temperature.

In order to obtain a resistivity difference between two specimens, one pair of specimens was mounted on a copper disc 38 mm in diameter and 13 mm in thickness, attached to

a helium pot in a stainless steel vacuum can. The copper disc was electrically insulated with thin adhesive polyester tape. The vacuum can was filled with 1 atm helium gas. The cryostat was spontaneously warmed from 4.2 to 80 K over about 30 h to maintain a uniform temperature distribution in the copper disc. Temperatures were monitored with a thermocouple of Au–0.07 at.% Fe versus chromel placed between the pair of specimens, and a thermal EMF was measured with a digital voltmeter within a measurement error of ±0.07 K. A resistance ratio between the pair of specimens at temperatures 4.2–80 K was measured on a bridge circuit composed of the pair: one of the pair as a reference specimen R_1 and the other as an unknown specimen R_2. A small potential difference ΔV between these specimens was measured with a DC comparator potentiometer with a resolution of ±0.5 nV (Guildline, Model 9930). The resistance ratio was determined from the relation $R_2/R_1 = (I_1/I_2)[1 + \Delta V/(I_1R_1)]$, where I_1 and I_2 are the currents through R_1 and R_2, respectively. The specimen with the ⟨111⟩ axis was used as the reference specimen. The size factor $\alpha(\equiv A/l_p)$ was determined from the relation $\alpha = \rho/R$ using a measured value of R(300 K) and a value of 27.33 nΩ m for ρ(300 K) [9]. Here, A is the sectional area of the specimen and l_p the distance between potential electrodes. The thickness d was determined from the relation $d = (l_p/w)\alpha$, where w is the width of the specimen. Specifications of the present specimens are listed in table 1.

Table 1. Specifications of the specimens in sets A and B: the crystallographic orientation of the *specimen axis [hkl], the thickness d, the width w, the distance between potential electrodes* l_p, the measured resistivity ρ(4.2 K), the size-corrected resistivity ρ_b(4.2 K) and the extrapolated resistivity $\rho(0)$ at $T = 0$ K. The surface orientation $(1\bar{1}0)$ is common to all the specimens.

Specimen	[*hkl*]	*d* (mm)	*w* (mm)	l_p (mm)	ρ(4.2 K)[a] (pΩ m)	ρ_b(4.2 K)[b] (pΩ m)	$\rho(0)$ (pΩ m)
A1	[110]	0.428	2.954±0.003	8.06±0.01	1.401±0.003	0.473	1.43
A2	[111]	0.469	2.983±0.005	20.04±0.01	1.44±0.03	0.56	1.32
A3	[001]	0.331	2.857±0.011	15.19±0.01	1.88±0.03	0.69	1.72
B1	[110]	0.421	3.049±0.004	8.38±0.01	1.402±0.003	0.467	1.31
B2	[111]	0.558	3.049±0.004	12.69±0.01	1.312±0.003	0.544	1.24
B3	[001]	0.457	3.062±0.003	12.13±0.01	1.636±0.003	0.716	1.54

[a] Values obtained by the direct current comparator potentiometer are listed for specimens A2 and A3, and those obtained by the superconducting chopper amplifier for specimens A1, B1, B2 and B3.
[b] Values estimated according to the Fuchs–Sondheimer theory assuming that $p = 0$ and $\rho_b l_b = 0.82$ fΩ m^2.

In order to obtain the temperature-dependent part $\rho^{ph}(T)$ of the resistivity, the residual part $\rho(0)$ was subtracted from the total resistivity $\rho(T)$ $(= \rho(0)+\rho^{ph}(T))$. The value of $\rho(0)$ was determined by the least-mean-squares fitting of a polynomial, $A_0+A_2T^2+A_3T^3+A_5T^5$, to the data of $\rho(T)$ obtained below 15 K. The value of $\rho(0)$ $(= A_0)$ is listed in table 1. Here, it should be noted that a contribution to the resistivity from the surface scattering, as well as the contribution from impurities and other defects, is already subtracted for $\rho^{ph}(T)$. The ratios $\rho^{ph}_{100}(T)/\rho^{ph}_{111}(T)$ and $\rho^{ph}_{110}(T)/\rho^{ph}_{111}(T)$ are shown in figures 2 and 3 for the specimens in sets A and B, respectively, where $\rho^{ph}_{hkl}(T)$ means $\rho^{ph}(T)$ in a specimen with the ⟨*hkl*⟩ axis. The deviation of the ratios from 1.0 represents the anisotropy of the temperature dependence of resistivity. The reproducibility of the measurement is good. The behaviour of $\rho^{ph}(T)$ is similar to the total resistivity $\rho(T)$ [1].

A remarkable anisotropy is observed in the temperature-dependent part $\rho^{ph}(T)$ at low temperatures. At temperatures below about 25 K, $\rho^{ph}_{100}(T)$ is larger than $\rho^{ph}_{111}(T)$, but

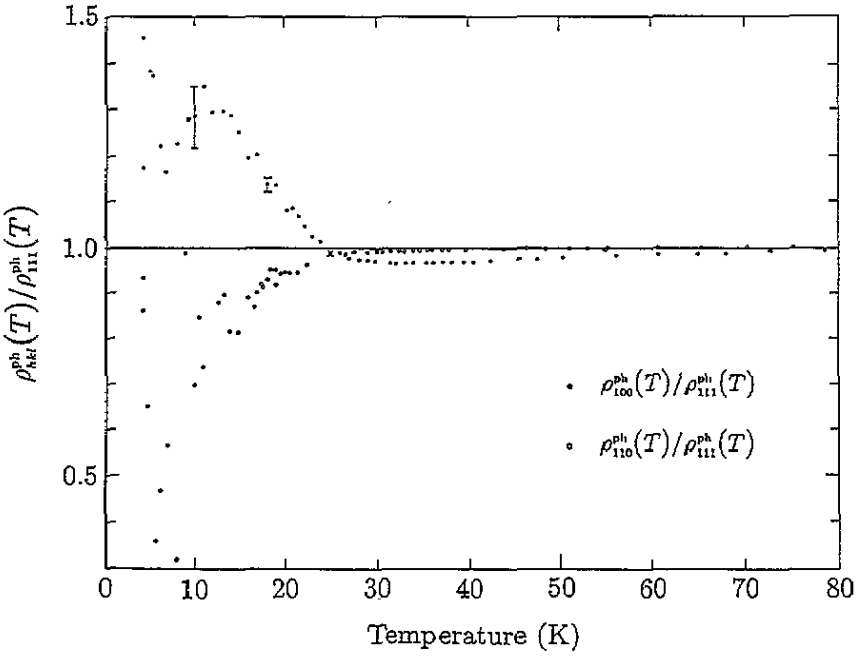

Figure 2. Ratios of the temperature-dependent part of the electrical resistivity $\rho^{ph}_{hkl}(T)$ to $\rho^{ph}_{111}(T)$ as a function of temperature for the aluminium single-crystal specimens with the $\langle hkl \rangle$ axis in set A.

$\rho^{ph}_{110}(T)$ is, in contrast, smaller than the latter: $\rho^{ph}_{100}(T) > \rho^{ph}_{111}(T) > \rho^{ph}_{110}(T)$. In this temperature region, $\rho^{ph}(T)$ has the larger value in the order of symmetry of the specimen axis. These features are the same as those of ρ_b(4.2 K) reported previously [1]. The ratio $\rho^{ph}_{110}(T)/\rho^{ph}_{111}(T)$ rapidly approaches 1.0 with increasing temperature. On the other hand, the ratio $\rho^{ph}_{100}(T)/\rho^{ph}_{111}(T)$ approximates to 1.0 at about 25 K and takes the minimum value between 30 and 35 K. Then, it gradually approaches 1.0 at higher temperatures. The relative difference of $\rho^{ph}(T)$ between specimens with the different axis orientation is large at temperatures below 20 K, and this large anisotropy seems to persist even in the lowest temperature region, although the data are scattered.

The behaviour of the anisotropy of $\rho^{ph}(T)$ described above shows a good correspondence with that of ρ(4.2 K) as a function of $P/2A$ in figure 1. The anisotropy of $\rho^{ph}(T)$ in the region $T < 25$ K, where the rate of the electron–phonon scattering is small, is the same as that of ρ(4.2 K) in the region $P/2A < 3 \times 10^3$ m^{-1}. In the region $T >$ 25 K, where the scattering rate is large, the anisotropy of $\rho^{ph}(T)$ decreases similarly to that of ρ(4.2 K) in the region $P/2A > 4 \times 10^3$ m^{-1}.

In high-purity aluminium for the present experiment, the electron–impurity scattering is largely reduced. Eventually, the anisotropic electron–phonon scattering at low temperatures and the electron–electron scattering relatively increase their influence on the electrical resistivity. In fact, $\rho^{ph}(T)$ in the present specimens deviates from the Bloch–Grüneisen expression [10] at temperatures below 20 K where the anisotropy of $\rho^{ph}(T)$ is remarkable. In aluminium, the second-zone Fermi surface is nearest to the Brillouin zone boundary that is perpendicular to the high-symmetric direction ⟨100⟩. Moreover, it contacts with the third-zone Fermi surface near the W point. When an electric field is applied in the ⟨100⟩

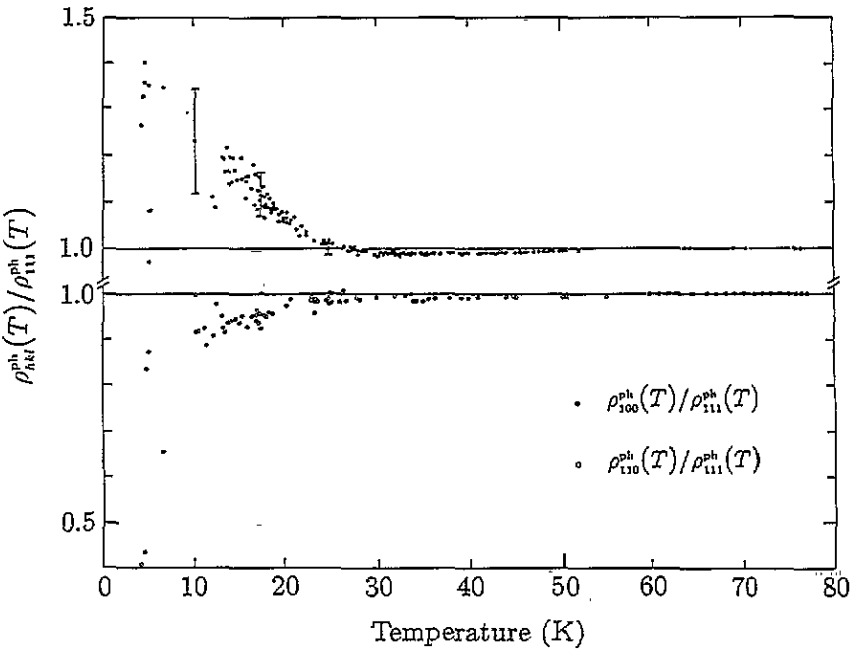

Figure 3. Ratios of $\rho^{ph}_{hkl}(T)$ to $\rho^{ph}_{111}(T)$ as a function of temperature for the aluminium single-crystal specimens in set B.

direction, the electron distribution deviates from the equilibrium in this direction towards the zone boundary. A possible suggestion to explain the anisotropy of $\rho^{ph}(T)$ is that the probability of the Umklapp process is enhanced due to this deviation of electron distribution by the electric field along ⟨100⟩. When the temperature is raised over 20 K, the scattering rate of electrons due to the normal process increases and the electron distribution will be homogenized. Then, the anisotropy of $\rho^{ph}(T)$ will decrease. The change in the process of electron–phonon scattering will be a cause of the detailed behaviour of $\rho^{ph}_{100}(T)/\rho^{ph}_{111}(T)$ in figures 2 and 3 that shows the minimum between 30 and 35 K. The mechanism of the anisotropy that works in $\rho^{ph}(T)$ may relate to that of the residual resistivity. Further investigations, both experimental and theoretical, are needed to elucidate the mechanism of this anisotropy of the electrical resistivity.

References

[1] Hashimoto E, Ueda Y, Tamura H and Kino T 1993 *J. Phys. Soc. Japan* **62** 4178
[2] Sondheimer E H 1952 *Adv. Phys.* **1** 1
[3] Sambles J R, Elsom K C and Sharp-Dent G 1981 *J. Phys. F: Met. Phys.* **11** 1075
[4] Ueda Y, Hosoda H and Kino T 1985 *J. Phys. Soc. Japan* **54** 3858
[5] Sato H and Yonemitsu K 1976 *Phys. Status Solidi* b **73** 723
[6] Rossiter P L 1986 *The Electrical Resistivity of Metals and Alloys* (Cambridge: Cambridge University Press) ch 1
[7] Ueda Y, Hosoda H and Kino T 1988 *J. Phys. Soc. Japan* **57** 3896
[8] Ribot J H J M, Bass J, van Kempen J H, van Vucht R J M and Wyder P 1981 *Phys. Rev.* B **23** 532
[9] Kawata S and Kino T 1975 *J. Phys. Soc. Japan* **57** 3896
[10] Ziman J M 1960 *Electrons and Phonons* (London: Oxford University Press) ch 9